Gapless superconductivity in ferromagnet/superconductor junctions

Guoya Sun, D. Y. Xing,* and Jinming Dong
National Laboratory of Solid State Microstructures and Department of Physics, Nanjing University, Nanjing 210093, China

Mei Liu
Department of Physics, Southeast University, Nanjing 210096, China

(Received 10 October 2001; published 16 April 2002)

The Nambu spinor Green's function approach is applied to study the proximity effect in ferromagnet/superconductor (FM/SC) junctions. It is found that gapless superconductivity appears in both FM and SC regions near the FM/SC interface. In FM the superconducting order parameter induced by the proximity effect displays a damped oscillation. When the distance from the interface increased, following a transition from the ''0 state'' to the ''π state,'' the induced superconducting density of states in FM is flipped with respect to the normal state. Quantitative agreement is obtained between the calculated results and recent tunneling spectra in $Al/Al_2O_3/PbNi/Nb$ tunnel junctions. In particular, peak and dip behavior of the induced superconducting DOS in FM is well reproduced.

DOI: 10.1103/PhysRevB.65.174508 PACS number(s): 74.50.+r, 74.80.Fp

I. INTRODUCTION

The coexistence of superconductivity and ferromagnetism has been a most interesting subject in condensed matter physics.[1–13] Early in the 1960's Fulde and Ferrel[1] and Larkin and Ovchinnikov[2] (FFLO) predicted that pairing can still occur when electron momenta at the Fermi energy are different for two spin directions, for instance, as the result of an exchange field in magnetic superconductors. Unlike the conventional Cooper pair, in which two electrons have opposite spins and momenta $(\mathbf{k}\uparrow,-\mathbf{k}\downarrow)$, the ''FFLO'' pairing in the presence of an exchange field has a finite center-of-mass momentum $Q=2h_0/\hbar v_F$ and consequently leads to a spatially modulated superconducting order parameter, where $2h_0$ is the exchange energy corresponding to the difference in energy between the spin-up and spin-down bands, and v_F is the Fermi velocity. The ''FFLO'' state with $[(\mathbf{k}+\mathbf{Q}/2)\uparrow,(-\mathbf{k}+\mathbf{Q}/2)\downarrow]$ was never observed in bulk materials. This stems from the fact that in a bulk ferromagnet (FM) h_0 is typically at least 2 orders of magnitude larger than the energy gap Δ_0 of a bulk superconductor (SC), while the normal state is recovered as soon as $2h_0$ exceeds $\sqrt{2}\Delta_0$, which is called the Clogston criterion.[3] However, this criterion may be largely relaxed if Cooper pairs are injected from an SC into an FM by the proximity effect. Very recently, Kontos *et al.*[9] and Ryazanov *et al.*[10] have shown that inhomogeneous superconductivity can be induced in FM by the proximity effect in FM/SC nanostructures, even though h_0 in FM is much greater than Δ_0 in SC.

It is well known that the superconducting order parameter and energy gap are two different concepts. The order parameter describes the number of Cooper pairs in the condensate and determines the basic features of superconductors: the Meissner effect and the absence of electric resistance; while the energy gap is the minimum binding energy of the Cooper pairs, which manifests itself in the low-temperature heat capacity, thermal conductivity, absorption of electromagnetic radiation, and ultrasound, etc.[14] A typical example of the distinction between them is the gapless superconductivity observed in superconductors containing magnetic impurities, where there is a finite superconducting order parameter but a vanishing energy gap. In this case, the Bose condensate of the Cooper pairs does not contain all the pairs due to the pair-breaking effect of magnetic impurities, the order parameter describes the coherent wave function of the condensate pairs, while the energy gap may vanish. In reality, the magnetic impurities do not provide the only pair-breaking mechanism. The same effect is exhibited by any perturbations giving rise to time-reversal symmetry breaking terms in the Hamiltonian. As will be shown in this work, the proximity effect in an FM/SC junction leads to gapless superconductivity not only on the FM side due to the injection of Cooper pairs, but also on the SC side due to the injection of spin-polarized electrons.

In this work we first extend the theoretical approach of normal-metal/SC junction systems developed by McMillan[15] and Blonder, Tinkham, and Klapwijk (BTK)[16] to an FM/SC junction, from which wave functions of quasiparticles on both FM and SC sides can be obtained. Then, we construct 2×2 spinor Green's functions in the Nambu representation.[17] The superconducting order parameter is described by the imaginary part of its off-diagonal component. The density of states (DOS) near the Fermi level is proportional to the imaginary part of its diagonal component. It is found that with increasing the distance from the FM/SC interface, the superconducting order parameter in the FM decreases and its sign reverses from positive to negative, corresponding to a transition from the ''0 state'' to ''π state.'' The induced superconducting DOS decreases gradually with increasing the distance from the FM/SC interface and is flipped with respect to the normal state following the transition from the ''0 state'' to ''π state.'' This result is consistent with the differential conductance spectra observed recently in $Al/Al_2O_3/PdNi/Nb$ tunnel junctions.[9] In that experiment the most important point is the reversed change in the DOS having a superconducting feature with increasing thickness of the FM layer, in particular, the peak in DOS at $E=\Delta_0$ for the ''0 state'' and the dip in the DOS at the same energy for

the ''π state'' where Δ_0 is the energy gap in bulk SC. Zareyan, Belzig, and Nazarov[11] have used a quasiclassical approach based on the Eilenberger equation in the clean limit to reproduce the shape of DOS observed in either the ''0'' or ''π state.'' Their theoretical fit to the experiment was focused on the range of $E<\Delta_0$, while the DOS in FM was measured in the range of $E<4\Delta_0$. In the present work, good agreement between theory and experiment[9] is obtained in the whole range of measurements, including the peak and dip behavior of the induced superconducting DOS at $E=\Delta_0$ in the FM layer. At the same time, it is found that gapless superconductivity in the SC exists near the FM/SC interface due to the injection of spin-polarized electrons. On the FM side, the superconducting DOS induced by the proximity effect is also gapless.

II. MODEL AND THEORY

We consider the planar semi-infinite geometry with an FM to the left of $x=0$ and an SC to the right. The FM/SC interface at $x=0$ is described by a δ-type barrier potential $V(x)=U\delta(x)$, where U depends on the product of the barrier height and width. The FM is described by an effective single-particle Hamiltonian for spin-polarized electrons, the SC is assumed s-wave pairing and described by a BCS-like Hamiltonian. Owing to the interplay between them near the interface the superconducting properties should be determined in a self-consistent way. We begin with a reasonable guess for the potentials in both regions while remembering that they should be determined self-consistently. In the one-dimensional BTK model,[16] the quasiparticle wave function satisfies the following BdG equation:

$$\begin{bmatrix} H_0(x)-\eta_\sigma h(x) & \Delta(x) \\ \Delta^\star(x) & -H_0(x)-\eta_\sigma h(x) \end{bmatrix} \begin{bmatrix} u_\sigma \\ v_{\bar\sigma} \end{bmatrix} = E \begin{bmatrix} u_\sigma \\ v_{\bar\sigma} \end{bmatrix}. \tag{1}$$

Here $H_0(x)=-(\hbar^2/2m)\nabla_x^2+V(x)-E_F$ and E is the quasiparticle energy relative to the Fermi energy E_F. $h(x)=h_0\Theta(-x)$ is the exchange energy in the FM with $\Theta(x)$ is the unit step function. $\eta_\sigma=1$ for $\sigma=\uparrow$ and -1 for $\sigma=\downarrow$, $\bar\sigma$ standing for the spin opposite to σ. As the first guess for the self-consistent BCS pair potential, we choose $\Delta(x)=\Delta_0\Theta(x)$. In Eq. (1) the spin-flip process has been neglected in the SC near the interface, and as a result, the spin-dependent (four-component) BdG equation may be decoupled into two sets of two-component equations: $(u_\sigma, v_{\bar\sigma})$ describing the spin-σ electronlike quasiparticle (ELQ) and spin-$\bar\sigma$ holelike quasiparticle (HLQ) with $\sigma=\uparrow$ and $\downarrow$.[8] Following the standard method developed by McMillan,[15] we employ two envelop functions $\bar{u}_\sigma(x)$ and $\bar{v}_{\bar\sigma}(x)$ which are defined by $\bar{u}_\sigma(x)=u_\sigma(x)\exp(-ik_F^\sigma x)$ and $\bar{v}_{\bar\sigma}(x)=v_{\bar\sigma}(x)\exp(-ik_F^{\bar\sigma}x)$, where $k_F^\sigma=k_F\sqrt{1+\eta_\sigma h(x)/E_F}$, $\bar{u}_\sigma(x)$ and $\bar{v}_{\bar\sigma}(x)$ are smooth on the atomic scale length. Substituting $\bar{u}_\sigma(x)$ and $\bar{v}_{\bar\sigma}(x)$ into Eq. (1) and dropping the d^2/dx^2 term which is of order Δ_0/E_F with respect to the d/dx term, we obtain the reduced BdG equation as

$$\frac{-i\hbar^2k_F^\sigma}{m}\frac{d}{dx}\bar{u}_\sigma(x)+\bar{\Delta}^*(x)\bar{v}_{\bar\sigma}(x)=E\bar{u}_\sigma(x), \tag{2}$$

$$\frac{i\hbar^2k_F^{\bar\sigma}}{m}\frac{d}{dx}\bar{v}_{\bar\sigma}(x)+\bar{\Delta}(x)\bar{u}_\sigma(x)=E\bar{v}_{\bar\sigma}(x), \tag{3}$$

where $\bar{\Delta}(x)=\Delta(x)\exp[i(k_F^\sigma-k_F^{\bar\sigma})x]$. There are four types of quasiparticle injection processes at the FM/SC interface: electron and hole injection from FM to SC, and ELQ and HLQ injection from SC to FM. Consider a spin-σ electron incident on the interface at $x=0$ from the FM, there are four possible trajectories: normal reflection (b_1^σ), Andreev reflection ($a_1^{\bar\sigma}$), transmission to the SC as ELQ (c_1^σ), and transmission as HLQ ($d_1^{\bar\sigma}$). With general solutions of BdG equations (2) and (3), the wave functions in FM and SC regions are described by

$$\psi_{1\sigma}(x)=\begin{cases} \begin{pmatrix}1\\0\end{pmatrix}e^{ik_e^\sigma x}+a_1^{\bar\sigma}\begin{pmatrix}0\\1\end{pmatrix}e^{ik_h^{\bar\sigma}x}+b_1^\sigma\begin{pmatrix}1\\0\end{pmatrix}e^{-ik_e^\sigma x} & x\leqslant 0, \\ c_1^\sigma\begin{pmatrix}u\\v\end{pmatrix}e^{iq_e x}+d_1^{\bar\sigma}\begin{pmatrix}v\\u\end{pmatrix}e^{-iq_h x} & x\geqslant 0, \end{cases} \tag{4}$$

where $k_{e(h)}^\sigma=k_F^\sigma+(-)mE/\hbar^2k_F^\sigma$, $q_{e(h)}=k_F+(-)m\Omega/\hbar^2k_F$, $u=\sqrt{(1+\Omega/E)/2}$, and $v=\sqrt{(1-\Omega/E)/2}$ with $\Omega=\sqrt{E^2-\Delta_0^2}$. All the coefficients $a_1^{\bar\sigma}$, b_1^σ, c_1^σ, and $d_1^{\bar\sigma}$ can be determined by matching the boundary conditions at $x=0$: $\psi_{1\sigma}(0_-)=\psi_{1\sigma}(0_+)$ and $[d\psi_{1\sigma}(x)/dx]_{x=0_-}=[d\psi_{1\sigma}(x)/dx]_{x=0_+}+2k_FZ\psi_{1\sigma}(0)$, where $Z=mU/(\hbar^2k_F)$ is the dimensionless barrier strength. The wave functions for the other three types of quasiparticle injection processes can be obtained in a similar way.

In what follows we calculate the Nambu spinor Green's functions in the FM/SC structure. With the wave functions $\psi_{i\sigma}(x)$ ($i=1,\ldots,4$ and $\sigma=\uparrow,\downarrow$), the retarded Green's function is constructed from a linear combination of them:[18] $G_r^\sigma(x,x',E)=\alpha_1^\sigma\psi_{3\sigma}(x)\hat{\psi}_{1\sigma}^t(x')+\alpha_2^\sigma\psi_{3\sigma}(x)\hat{\psi}_{2\sigma}^t(x')+\alpha_3^\sigma\psi_{4\sigma}(x)\hat{\psi}_{1\sigma}^t(x')+\alpha_4^\sigma\psi_{4\sigma}(x)\hat{\psi}_{2\sigma}^t(x')$ for $x\leqslant x'$, and $\beta_1^\sigma\psi_{1\sigma}(x)\hat{\psi}_{3\sigma}^t(x')+\beta_2^\sigma\psi_{2\sigma}(x)\hat{\psi}_{3\sigma}^t(x')+\beta_3^\sigma\psi_{1\sigma}(x)\hat{\psi}_{4\sigma}^t(x')+\beta_4^\sigma\psi_{2\sigma}(x)\hat{\psi}_{4\sigma}^t(x')$ for $x\geqslant x'$, where the wave function $\hat{\psi}_{i\sigma}(x)$ is conjugate to $\psi_{i\sigma}(x)$ and $\hat{\psi}_{i\sigma}^t(x)$ is the transposition of $\hat{\psi}_{i\sigma}(x)$. The coefficients α_i^σ and β_i^σ ($i=1,\ldots,4$) are determined by satisfying the following equations: $G_r^\sigma(x,x+0_+,E)=G_r^\sigma(x,x-0_+,E)$ and $\partial G_r^\sigma(x,x',E)/\partial x|_{x=x'+0_+}-\partial G_r^\sigma(x,x',E)/\partial x|_{x=x'-0_+}=(2m/\hbar^2)\hat{\tau}_3$, where $\hat{\tau}_3$ is the Pauli matrix. After carrying out a little tedious calculation, we get the Green's functions as

$$\begin{aligned} G_r^\sigma(x,x,E)=&-\frac{im}{\hbar^2k_e^\sigma}\left[(1+b_1^\sigma e^{-2ik_e^\sigma x})\begin{pmatrix}1&0\\0&0\end{pmatrix}\right. \\ &\left.+a_1^{\bar\sigma}e^{i(k_h^{\bar\sigma}-k_e^\sigma)x}\begin{pmatrix}0&0\\1&0\end{pmatrix}\right]-\frac{im}{\hbar^2k_h^{\bar\sigma}}\left[(1+a_2^{\bar\sigma}e^{2ik_h^{\bar\sigma}x})\right. \\ &\left.\times\begin{pmatrix}0&0\\0&1\end{pmatrix}+b_2^\sigma e^{i(k_h^{\bar\sigma}-k_e^\sigma)x}\begin{pmatrix}0&1\\0&0\end{pmatrix}\right] \end{aligned} \tag{5}$$

in the FM and

$$G_r^{\sigma}(x,x,E) = -\frac{imE}{\hbar^2 q_e q_h \Omega}\left[q_h(1+b_3^{\sigma}e^{2iq_e x})\begin{pmatrix} u^2 & uv \\ uv & v^2 \end{pmatrix} + q_e b_4^{\sigma} e^{i(q_e-q_h)x}\begin{pmatrix} uv & v^2 \\ u^2 & uv \end{pmatrix}\right] - \frac{imE}{\hbar^2 q_h q_e \Omega} \times\left[q_e(1+\bar{a_4^{\sigma}}e^{-2iq_h x})\begin{pmatrix} v^2 & uv \\ uv & u^2 \end{pmatrix} + q_h \bar{a_3^{\sigma}} e^{i(q_e-q_h)x}\begin{pmatrix} uv & u^2 \\ v^2 & uv \end{pmatrix}\right] \quad (6)$$

in the SC, where the expressions for sixteen coefficients are given in the Appendix.

The local DOS of the quasiparticles is proportional to the imaginary part of the 11 component of the 2×2 retarded Green function ($x=x'$),

$$N(x,E) = (-1/\pi)\sum_{\sigma} \mathrm{Im}[G_r^{\sigma}(x,x,E)]_{11}. \quad (7)$$

From the Green's function obtained above, the pair potential can be recalculated, yielding $\Delta(x)=\lambda^*(x)F(x)$, where $\lambda^*(x)=(\lambda-\mu^*)/(1+\lambda)$ with λ the dimensionless electron-phonon coupling constant and μ^* the Coulomb pseudopotential.[15] λ and μ^* are taken to be equal to the bulk value in the SC and zero in the FM. $F(x)$ is the superconducting order parameter, which is determined by the off-diagonal component of the Green's function ($x=x'$)

$$F(x) = (1/\pi)\sum_{\sigma} \int_0^{\infty} dE\, \mathrm{Im}[G_r^{\sigma}(x,x,E)]_{12}. \quad (8)$$

III. CALCULATION AND RESULTS

Figure 1 shows calculated results for spatial variation of the order parameter $F(x)$ in the FM/SC structure. On the FM side, the proximity effect induces the superconducting order parameter. Increasing the distance from the interface, $F(x)$ displays a damped oscillation and changes sign from positive to negative at $x\approx\xi_F$, where $\xi_F=\hbar v_F/2h_0$ is the coherence length in FM. As Cooper pairs are injected from SC to FM, they are not instantaneously broken and can survive for a time corresponding to a traveled length on the order of ξ_F. In the FM the spin-σ electron and spin-$\bar{\sigma}$ hole have a different Fermi momentum and their difference is equal to $\hbar k_e^{\sigma} - \hbar k_q^{\bar{\sigma}} \simeq 2h_0/\hbar v_F = Q$. The interference between the electron and hole wave functions produces an oscillating term of $\exp(ix/\xi_F)$ with $\xi_F=1/Q$ (Refs. 6,19) in the off-diagonal component of Eq. (5). Correspondingly, the momentum difference, either between ELQ and HLQ in the SC or between the electron and hole in the normal metal ($h_0=0$), is only the order of $2\Delta_0/\hbar v_F$ and so the coherence length in SC is equal to $\xi_S=\hbar v_F/2\Delta_0$. It then follows that ξ_F is much shorter than ξ_S and the ratio ξ_F/ξ_S is equal to about Δ_0/h_0. As a result, $F(x)$ in an FM/SC junction has a much shorter oscillating period and much smaller oscillation damping compared with that in a normal-metal/SC junction. Usually, the states corresponding to a positive sign of $F(x)$ are called the "0 state" and those corresponding to a negative sign of $F(x)$ called the "π state." A transition from the "0 state" to the "π state" is clearly shown in Fig. 1. On the SC side, the order parameter is diminished near the FM/SC interface. It recovers its bulk value as the distance from the interface exceeds the coherent length ξ_S, The recalculated pair potential $\Delta(x)$ in the SC is equal to the bulk λ^* times $F(x\geqslant 0)$ given in Fig. 1, and that in the FM is zero because $\lambda^*=0$ there. This potential is not very different from the assumed one $\Delta(x)=\Delta_0\Theta(x)$, indicating that the potential is now nearly self-consistent.

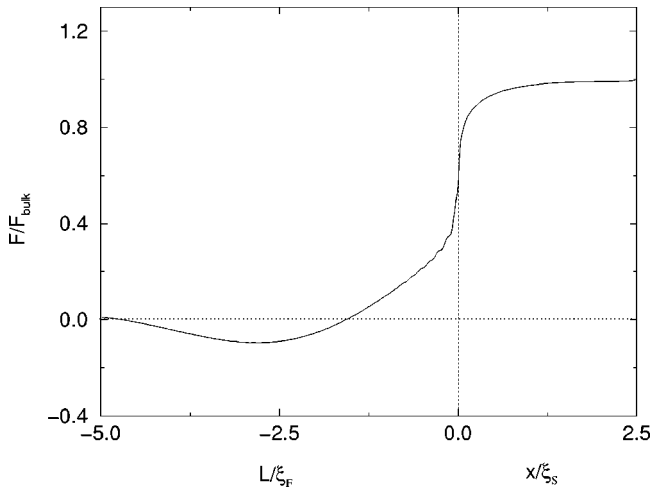

FIG. 1. Spatial variation of superconducting order parameter $F(x)$ in FM and SC. Here $\xi_F=\hbar v_F/2h_0$ and $\xi_S=\hbar v_F/2\Delta_0$ with $E_F=1000\Delta_0=1.4$ eV, $h_0=15$ meV, and $Z=0.3$ taken.

In Fig. 2(a), we plot spatial variation of the DOS of quasiparticles in FM, in which the DOS has been normalized by that when the SC is at its normal state. In PbNi alloys with 10% of Ni, the ferromagnetic exchange energy is taken to be 15 meV, resulting $\xi_F\approx 40$ Å. It is found that at $|x|=50$ Å the superconducting order parameter is positive ("0 state") and the DOS displays a maximum at the energy-gap edge ($E=\Delta_0$) and a minimum at the Fermi level ($E=0$), exhibiting a SC-like shape. With increasing the distance from the interface, the SC-like behavior of the DOS disappears gradually. At $|x|=75$ Å the maximal DOS appears at $E=0$ and the minimal DOS at the gap edge for the "π state." Such two different DOS shapes for the "0" and "π" states have been recently observed in the tunneling conductance spectra for two $Al/Al_2O_3/PbNi/Nb$ tunnel junctions corresponding to two different thicknesses ($L=50$ and 75 Å) of PbNi.[9] The measured tunneling spectra there correspond to the DOS of the PbNi film of thickness L at the $Al_2O_3/PbNi$ interface, they also correspond to the DOS of FM at $x=-L$ in the present FM/SC junction system. Quantitative agreement between the calculated results (solid lines) and experimental data (dotted lines) is shown in Fig. 2(a), where $Z=0.3$ is taken. The barrier strength is the only adjustable parameter in the present calculations. This choice of small Z indicates

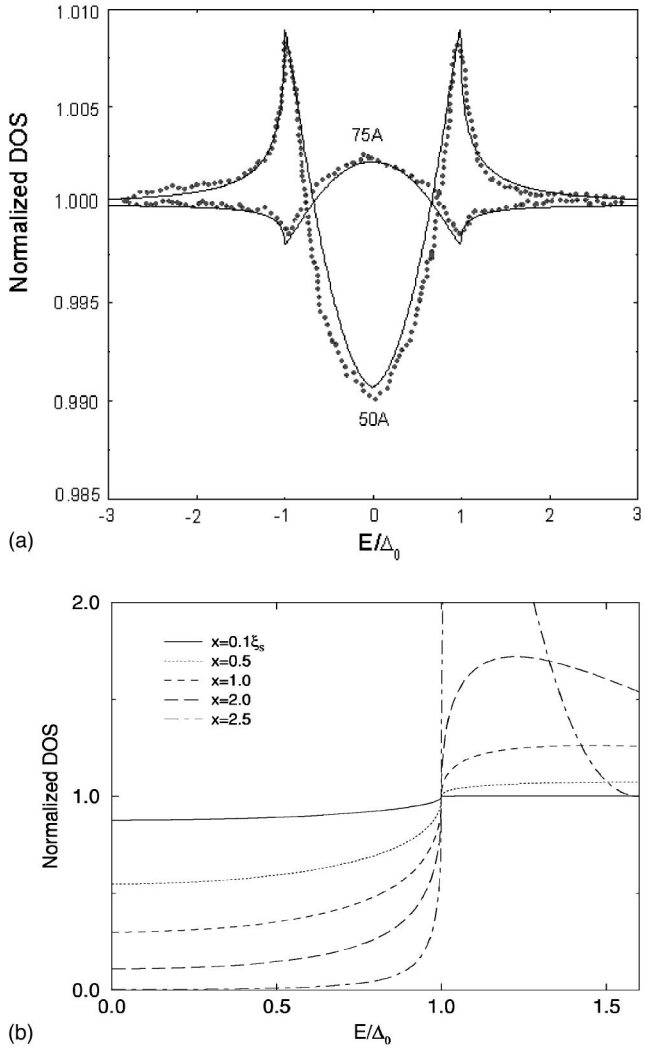

FIG. 2. Spatial variation of electronic DOS in FM (A) and SC (B). Following a transition from the "0 state" at $x=-50$ Å to the "π state" at $x=-75$ Å, the induced superconducting DOS (solid and dotted lines indicating calculated and experimental results, respectively) is flipped with respect to the normal state. There is gapless superconductivity for $x<2.5\xi_S$.

weak barrier strength and is consistent with very low FM/SC interface resistances.[9] As shown in Fig. 2(a), a good agreement between theory and experiment is obtained in the whole range of measurement ($E<4\Delta_0$). In particular, the peak and dip behavior of the induced superconducting DOS at $E=\Delta_0$ is also reproduced, which is the most remarkable feature observed in the experiment.[9] Both the oscillating $F(x)$ and induced superconducting DOS in FM arise from the quantum interference between injected electrons (holes) and Andreev reflected holes (electrons), rather than from the quantum size effects of the FM film of finite thickness. This proximity effect appears in the FM/SC structure, whether the FM is semi-infinite or finite. As a result, the present replacement of a semi-infinite FM with the finite FM film used in the experiment[9] is a reasonable approximation. The consideration of finite thickness would not change the present results. We wish to point out here that it is impossible to form intrinsic superconductivity in the FM, because h_0 is much higher than the energy gap of an SC. $F(x)$ in FM is induced by the proximity effect via the FM/SC interface. Such an induced order parameter may give rise to an SC-like DOS, but cannot open a superconducting energy gap in the FM. Therefore, the induced superconductivity in the FM is gapless.

On the other hand, owing to the proximity effect the superconductivity in the SC near the interface also becomes gapless, as shown in Fig. 2(b). The DOS at $x=0.1\xi_S$ has the biggest departure from the bulk behavior, but the SC-like shape still remains similar to the DOS curve at $x=50$ Å in Fig. 2(a). Since the scale of the ordinate in Fig. 2(b) is much larger than in Fig. 2(a), the SC-like shape is not easy to be distinguished. With the distance from the interface increased, the DOS at $E=0$ gradually decreases and almost vanishes at $x=2.5\xi_S$. With further increasing x, the opened energy gap increases and finally both the DOS and energy gap in the bulk SC are recovered. The damped gapless superconductivity in the SC arises from a pair-breaking mechanism due to the injection of spin-polarized electrons from FM to SC. The reason why the gapless-superconducting region can extend as far as $x=2.5\xi_S$ is that the FM/SC junction itself has a much stronger proximity effect on SC than a normal-metal/SC junction and that the proximity effect has been taken into full account in the present approach. The former plays a dominant role; the greater the exchange energy in FM, the stronger the proximity effect in SC. As regards the latter, there are several points of explanation. First, if strong barrier strength exists (large Z) at the FM/SC interface, the proximity effect would become weak. Second, the spin-flip effect of spin-polarized electrons injected into SC is also not considered. If the spin diffusion length is shorter than ξ_S or of the same order of magnitude as ξ_S, this effect should be taken into account and the gapless region in SC would be reduced. Third, only the normal injection of quasiparticles is considered in the present model. The normal injection always makes the greatest contribution to the proximity effect, no matter whether it is the injection of spin-polarized particles from FM to SC or that of Cooper pairs from SC to FM. The factors above make the proximity effect more or less overestimated.

Finally, we give a brief discussion on the disorder effect. In the present work as well as Ref. 11 the clean limit is taken by considering that the thickness of the FM layer is smaller than the elastic mean free path. The good agreement between the present theory and experiment indicates that either the clean limit used here is a good approximation suitable for the experiment or that the disorder due to impurity scattering and interface roughness is of no importance to the change in DOS due to the proximity effect. In our calculation it is found that the Andreev reflection plays an important role in the proximity effect in an FM/SC system. With increasing the barrier strength at the FM/SC interface, the Andreev effect is suppressed, so is the proximity effect. For the same reason, the disorder also gives rise to a reduction in the proximity effect, which is unfavorable to the appearance of the induced superconducting DOS in FM. The theoretical reproduction of experimental data[9] has been realized in Ref. 11

and in the present work. They are based on different approaches: quasiclassical and quantum-statistical, respectively, but both of them are in the same clean limit. To our knowledge, no theory in the dirty limit has been reported to reproduce the peak and dip behavior in DOS at $E=\Delta_0$. In the theoretical approach to an FM/SC system, which is based on the Usadel equation in the dirty limit,[12,13] a peak appears in the DOS on the FM side at $E=h_0$ rather than $E=\Delta_0$. Since h_0 is more than Δ_0, this peak behavior in DOS at $E=h_0$ obtained in the dirty limit is irrelative to that at $E=\Delta_0$ observed in the experiment.[9]

IV. SUMMARY

While most of the theoretical works on the FM/SC proximity effect are based on the quasiclassical approach (Usadel or Eilenberger equation), we develop a quantum-statistical approach based on pioneer works of the McMillan and BTK theories, in which the quantum effects including the Andreev reflection are well taken into account. The Nambu spinor Green's functions are calculated to obtain the density of states and the superconducting order parameters in FM/SC junctions. The injection of Cooper pairs from SC to FM leads to a damped oscillation of the superconducting order parameter in FM. The induced superconducting DOS is flipped with respect to the normal state follows a transition from the ''0 state'' to ''π state.'' This result can reproduce the tunneling conductance spectra in $Al/Al_2O_3/PbNi/Nb$ tunnel junctions corresponding to two different thicknesses of PbNi in the whole range of measurement ($E<4\Delta_0$), in particular the peak and dip behavior at $E=\Delta_0$. At the same time, the injection of spin-polarized electrons from FM to SC results in novel gapless superconductivity in SC near the interface.

ACKNOWLEDGMENTS

This work was supported by the National Natural Science Foundation of China under Grant No. 10174011.

APPENDIX: EXPRESSIONS FOR THE SIXTEEN COEFFICIENTS IN EQS. (5) AND (6)

$$a_1^{\bar{\sigma}}=2z_0k_e^{\sigma}/A, \tag{A1}$$

$$b_1^{\sigma}=[z_0^2-(z_1-k_e^{\sigma}+2ik_FZ)(z_2+k_h^{\bar{\sigma}}-2ik_FZ)]/A, \tag{A2}$$

$$a_2^{\bar{\sigma}}=[z_0^2-(z_2-k_h^{\bar{\sigma}}-2ik_FZ)(z_1+k_e^{\sigma}+2ik_FZ)]/A, \tag{A3}$$

$$b_2^{\sigma}=2z_0k_h^{\bar{\sigma}}/A, \tag{A4}$$

$$a_3^{\bar{\sigma}}=-2uvq_e(k_e^{\sigma}+k_h^{\bar{\sigma}})/B, \tag{A5}$$

$$b_3^{\sigma}=[(q_e+k_h^{\bar{\sigma}}+2ik_FZ)(k_e^{\sigma}-q_h-2ik_FZ)v^2 + (q_e-k_e^{\sigma}+2ik_FZ)(q_h+k_h^{\bar{\sigma}}+2ik_FZ)u^2]/B, \tag{A6}$$

$$a_4^{\sigma}=[(q_h+k_e^{\sigma}-2ik_FZ)(k_h^{\bar{\sigma}}-q_e+2ik_FZ)v^2 + (q_e+k_e^{\sigma}-2ik_FZ)(q_h-k_h^{\bar{\sigma}}-2ik_FZ)u^2]/B, \tag{A7}$$

$$b_4^{\sigma}=-2uvq_h(k_e^{\sigma}+k_h^{\bar{\sigma}})/B, \tag{A8}$$

with $z_0=(q_e+q_h)uv/(u^2-v^2)$, $z_1=(q_eu^2+q_hv^2)/(u^2-v^2)$, $z_2=(q_ev^2+q_hu^2)/(u^2-v^2)$, $A=(z_1+k_e^{\sigma}+2ik_FZ)\times(z_2+k_h^{\sigma}-2ik_FZ)-z_0^2$, and $B=(k_e^{\sigma}-q_h-2ik_FZ)(q_e-k_h^{\sigma}-2ik_FZ)v^2+(q_e+k_e^{\sigma}-2ik_FZ)(q_h+k_h^{\sigma}+2ik_FZ)u^2$.

*Corresponding author: dyxing@nju.edu.cn

[1] P. Fulde and A. Ferrel, Phys. Rev. **135**, A550 (1964).
[2] A. Larkin and Y. Ovchinnikov, Sov. Phys. JETP **20**, 762 (1965).
[3] M.A. Clogston, Phys. Rev. Lett. **9**, 266 (1962).
[4] A.I. Buzdin and M.V. Kuprianov, JETP Lett. **52**, 487 (1990).
[5] Z. Radovic, M. Ledvij, L. Dobrosavljevic'-Grujic', A.I. Buzdin, and J.R. Clem, Phys. Rev. B **44**, 759 (1991).
[6] E.A. Demler, G.B. Arnold, and M.R. Beasley, Phys. Rev. B **55**, 15 174 (1997).
[7] I. Baladie, A. Buzdin, N. Ryzhanova, and A. Vedyayev, Phys. Rev. B **63**, 054518 (2001).
[8] Z.M. Zheng, D.Y. Xing, G.Y. Sun, and J.M. Dong, Phys. Rev. B **62**, 14 326 (2000); G.Y. Sun, Z.M. Zheng, D.Y. Xing, J.M. Dong, and Z.D. Wang, J. Phys.: Condens. Matter **13**, 627 (2001).
[9] T. Kontos, M. Aprili, J. Lesueur, and X. Grison, Phys. Rev. Lett. **86**, 304 (2001).
[10] V.V. Ryazanov, V.A. Oboznov, A.Yu. Rusanov, A.V. Veretennikov, A.A. Golubov, and J. Aarts, Phys. Rev. Lett. **86**, 2427 (2001).
[11] M. Zareyan, W. Belzig, and Yu.V. Nazarov, Phys. Rev. Lett. **86**, 308 (2001).
[12] A. Buzdin, Phys. Rev. B **62**, 11 377 (2000).
[13] R. Fazio and C. Lucheroni, Europhys. Lett. **45**, 707 (1999).
[14] A. A. Abrikosov, *Fundamentals of the Theory of Metal* (North-Holland, Amsterdam, 1988).
[15] W.L. McMillan, Phys. Rev. **175**, 559 (1968).
[16] G.E. Blonder, M. Tinkham, and T.M. Klapwijk, Phys. Rev. B **25**, 4515 (1982).
[17] Y. Nambu, Phys. Rev. **117**, 648 (1960).
[18] S. Kashiwaya and Y. Tanaka, Rep. Prog. Phys. **63**, 1641 (2000).
[19] A.V. Andreev, A. Buzdin, and R.M. Osgood III, Phys. Rev. B **43**, 10 124 (1991).